



## Positron annihilation study on polyaniline nanocomposite used for Pb(II) ion removal

N.J. Al-Thani<sup>a</sup>, J. Bhadra<sup>a,\*</sup>, D. Abdulmalik<sup>b</sup>, I. Al-Qaradawi<sup>b</sup>, A. Alashraf<sup>a</sup>, N.K. Madi<sup>a</sup>

<sup>a</sup>Center for Advanced Materials, Qatar University, Doha, Qatar, email: [n.al-thani@qu.edu.qa](mailto:n.al-thani@qu.edu.qa) (N.J. Al-Thani), Tel. +974 4033 5666; Fax: +974 4033 3989; emails: [jollybhadra@qu.edu.qa](mailto:jollybhadra@qu.edu.qa) (J. Bhadra), [aa.ashraf@qu.edu.qa](mailto:aa.ashraf@qu.edu.qa) (A. Alashraf), [cam@qu.edu.qa](mailto:cam@qu.edu.qa) (N.K. Madi)

<sup>b</sup>Physics Program, Qatar University, Doha, Qatar, emails: [d.malik@qu.edu.qa](mailto:d.malik@qu.edu.qa) (D. Abdulmalik), [ilham@qu.edu.qa](mailto:ilham@qu.edu.qa) (I. Al-Qaradawi)

Received 27 December 2015; Accepted 10 March 2016

---

### ABSTRACT

Nanocomposites of polyaniline (PANI) with three different concentrations of micrometre-sized sawdust are prepared in aqueous media via chemical casting method at room temperature. Thereafter, the removal efficiency of the obtained composites for lead (Pb) ion from aqueous solutions is studied. The influence of sawdust concentrations on chemical structure and morphology of the composites is investigated by Fourier transform infrared spectroscopy and scanning electron microscopy. In order to investigate the removal efficiency of nanocomposites, a number of studies are performed, such as influence of pH, contact time, metal loading and nanocomposite concentrations. Our investigation suggests that the optimum conditions to obtain the highest efficiency are 5% of sawdust in nanocomposite, pH 5 and 3 min equilibrium time. A novel method of positron annihilation measurement is performed in order to study the mechanism behind adsorption of PANI and composites. Results obtained from positron annihilation are also consistent with that of adsorption experiments. Furthermore, the adsorption kinetic has been studied using the Langmuir adsorption isotherm and the Freundlich adsorption isotherm models; among the two models, Freundlich adsorption isotherm model is found to be better with respect to equilibrium aspect.

*Keywords:* Adsorption; Nanofibre; Polymer composites; Removal efficiency; Heavy metal

---

### 1. Introduction

Water pollution has continuously become a key threat to the ecosystem, especially in developing countries, due to the steep growth in industrialisation. Heavy metal ions, such as chromium (Cr), lead (Pb), cadmium, (Cd), mercury (Hg), zinc (Zn), nickel (Ni) and cobalt (Co) deposited in both surface water and ground water beyond the acceptable limit is highly

toxic to the human body. Lead is considered as one of the most toxic pollutants released into natural water bodies from the waste of several industrial activities, such as oil refining, metal plating and battery manufacturing [1]. The removal of these toxic metal ions from water is a major challenge for pollution control of water. Despite having numerous ways to separate Pb from water bodies, the adsorption process is usually preferred due to some of its versatile characteristics, such as low cost, easy preparation. Polymers,

---

\*Corresponding author.

polymer composites and nanocomposites have drawn significant interest from the research community in recent years and are successfully used as adsorbents for heavy metals [2,3]. There have been numerous attempts reported on the adsorption of metal ions by functionalised polymers based on amine derivatives, such as polyacrylonitrile fibres, ethylenediamine and polyacrylamides [4–6]. Furthermore, conductive polymers, such as polyaniline (PANI), polypyrrole (PPY) and polythiophene (PT), are used as ion exchangers and have attracted a wide range of research interests due to their extensive applications, such as rechargeable batteries [7], electromagnetic shielding, gas sensors and the removal of heavy metals [8–11]. PANI has several potential applications because of its unique electrical and optical properties [9]. However, the possible commercial applications of PANI are hindered by its lack of processability. To overcome this problem, various efforts have been made, such as the addition of side groups to the polymer backbone [12], polymer grafting to a non-conducting polymer [13], composites of conducting polymers [14] and copolymerisation [15,16]. In the recent years novel use of agricultural waste such as rice husk ash, wood sawdust and wheat straw have been successfully made to adsorb dyes and dye mixtures from effluent of textile industries [3,17–20]. Among the various cellulosic materials that have been studied, sawdust is commonly used as an adsorbent for heavy metal ions being agricultural by products with no economical values [21,22].

In this research, we present a novel approach to remove heavy metals from wastewater by PANI–sawdust (SW) nanocomposites. The properties of the PANI–sawdust nanocomposites, especially their Pb-ion adsorption property, are studied using several characterisation techniques. A novel technique of positron annihilation lifetime spectroscopy has been implemented to study the mechanism of adsorption on the surface of nanocomposites.

## 2. Materials and methods

This section describes the materials used in this experiment, method of preparation and methods adopted for the characterisation of polymer and polymer composites.

### 2.1. Materials

Materials used in this work are aniline (extra pure > 99%, Sigma-Aldrich), ammonium peroxydisulphate (APS) and sulphuric acid from BDH. All reagents

are used without any further purification.  $\text{Pb}(\text{NO}_3)_2$  salt is obtained from Sigma-Aldrich and distilled water is used in this work.

### 2.2. Sample preparation

#### 2.2.1. Preparation of PANI

PANI is obtained using dispersion polymerisation by a conventional method described in the literature [23,24]. The process of polymerisation is initiated by adding ammonium persulphate dropwise to the solution of aniline in aqueous HCl under constant stirring. The bath temperature is maintained at 0–5°C and pH 4. The reaction is retained under constant stirring for 24 h. The reaction mixture turns into a bluish green homogeneous mixture indicating the completion of the polymerisation reaction. The resulting precipitate is filtered and washed with deionised water and methanol until the filtrate becomes colourless to remove any oligomer or unreacted oxidant. The powder of PANI salt is dried under reduced pressure at 40°C for 24 h. In order to prepare PANI base, the PANI salt is first dissolved in NaOH solution (0.2 M) and stirred for 4 h. Then the base form of PANI is filtered and dried at 40°C for 24 h.

#### 2.2.2. Crushing and sieving sawdust

Sawdust powders are collected using a Retsch micro-sieve shaker with a pore size of 43  $\mu\text{m}$ . Then, the Retsch Cryomill is used in a nitrogen environment to crush sawdust and acquire very fine particles of approximately 5–14- $\mu\text{m}$  diameter, as is evident by the results of scanning electron microscopy (SEM) micrograph analysis (shown in Fig. 1).

#### 2.2.3. Preparation of PANI–sawdust composites

The PANI–sawdust composite preparation is accomplished using casting method, where mixtures of PANI base with three different weight percentages (10, 5 and 3%) of sawdust are constantly stirred in 20 ml of formic acid solution at room temperature for 4 h. The desired composites are stored in a Petri dish overnight to make them dry and they are further dried by heating the same at 50°C for 3 h.

### 2.3. Characterisation methods

The characterisation techniques used to characterise PANI and its composites are UV–vis spectroscopy, Fourier transform infrared spectroscopy (FTIR), SEM,

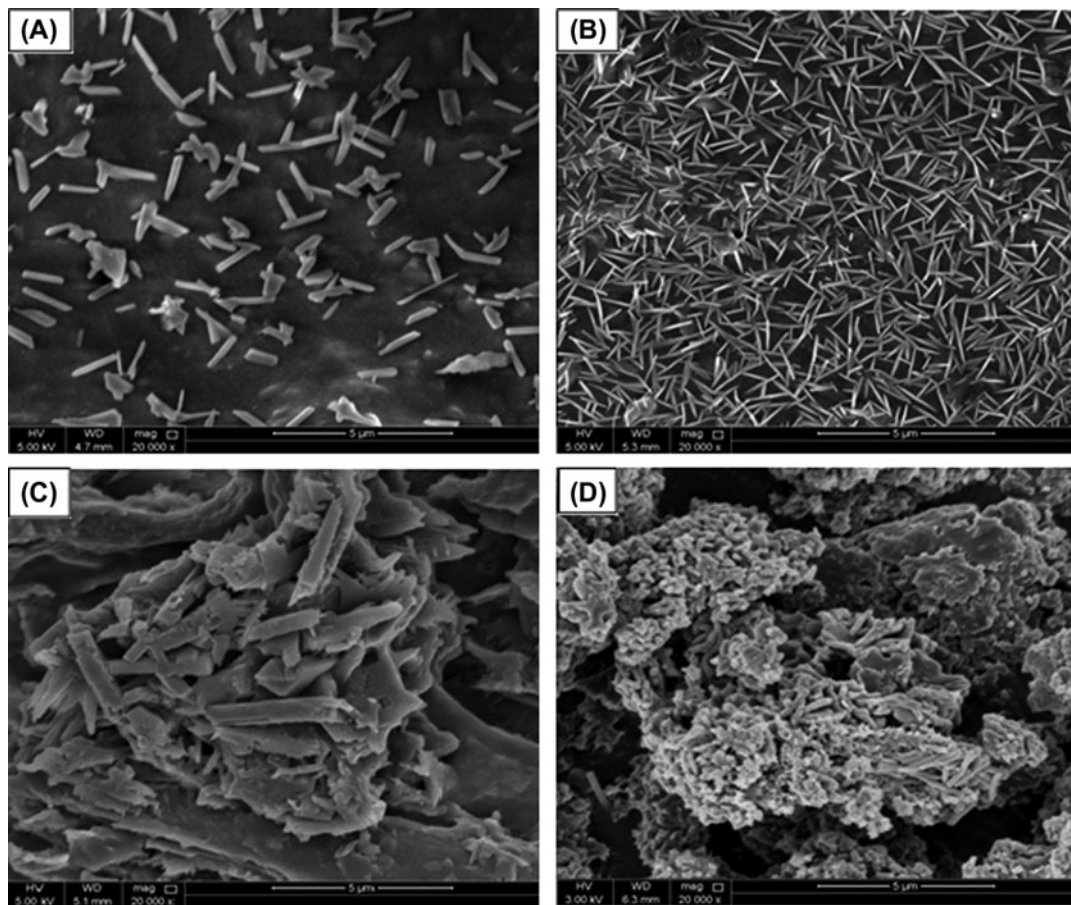


Fig. 1. SEM images of PANI-sawdust nanocomposites: (A) 3% sawdust, (B) 5% sawdust, (C) 10% sawdust and (D) pure PANI.

differential scanning calorimetry (DSC) and thermogravimetric analysis (TGA). UV-vis spectra are obtained using a Perkin Elmer Lambda EZ 210 spectrometer. SEM is performed to study the surface morphology, grain size of PANI and its composite using a Nano-SEM Nova 450 instrument. FTIR (8101 M, Shimadzu) is used for the study of chemical interaction between the polymers. To study the thermal properties of the PANI, TGA and DSC are performed using a Perkin Elmer Pyris TGA instrument and a Perkin Elmer Precisely Jade DSC instrument, respectively. Quantitative determination of Pb is performed using atomic absorption spectroscopy and inductively coupled-plasma atomic emission spectroscopy (ICP-MS). Positron lifetime spectroscopy is also used to probe any structural changes in the PANI and its composites by detecting vacancy-like defects formed in the material.

#### 2.4. Adsorption measurements

For the adsorption test, a glass column with dimension 1 cm × 10 cm (diameter and length,

respectively) equipped with a glass frit is employed for column adsorption experiments. A solution made of various concentrations (ppm) of Pb ion in distilled water obtained from lead nitrate salt is used as the synthetic polluted water for the test. The adsorption experiments are performed to study the effect of the experimental conditions on Pb adsorption and determine the conditions that lead to the maximum amount of Pb removal. The efficiency of Pb removal is calculated as follows:

$$\text{Removal \%} = \frac{C_i - C_f}{C_i} \times 100 \quad (1)$$

where  $C_i$  is the initial concentration (mg/L) and  $C_f$  is the final concentration (mg/L).

#### 2.5. Positron annihilation measurements

The PANI and its composites obtained in powdered form are compressed by conventional uniaxial

cold pressing at room temperature using Masada Jack to prepare cylindrical pellets of diameter 14 mm and thickness 2–25 mm under a pressure of 15–20 MPa.

### 2.5.1. Positron annihilation measurements

Positron lifetime measurements are performed using a fast–fast coincidence spectrometer with a time resolution (full width at half maximum) of 350 ps. The spectrometer consists of two plastic scintillation detectors and the related electronics for processing the signals and collecting the lifetime spectra. The measured samples are pure PANI, three PANI–sawdust composites with sawdust of different concentrations (3, 5 and 10%). The samples are measured before and after lead (Pb) extraction. The collected lifetime spectra are analysed using the LT 9 program [25]. The effect of the adsorption mechanism of Pb by PANI and its composites is investigated.

## 3. Results and discussion

### 3.1. SEM results

The morphological study of pure PANI and its sawdust composites performed by SEM are shown in Fig. 1(A)–(D). HCl-doped PANI shows predominantly fibrous morphology with fibres of uniform diameter of 93 nm. On the other hand, composites show some particle like morphology with variation in sawdust concentration. For the 3% sawdust composite, the sawdust particles are uniformly distributed in the PANI matrix and the composite particles are very loosely bonded because of low concentration. There is a decrease in pore size between the composite particles with increasing sawdust concentration, as can be observed in the SEM results. For the 10% sawdust composite, the particles are tightly bonded that may lead to reduction in adsorption sites of Pb. Among the three, 5% sawdust composites seem to have the optimum pore size necessary for adsorption process.

### 3.2. Infrared spectroscopy

A study on chemical interaction among the composite materials is executed by FTIR technique. Fig. 2 represents the FTIR spectra of pure PANI, pure sawdust and PANI–sawdust composites. The appearance of new peaks in the composites FTIR spectra, along with changes in existing peaks, directly indicates of chemical composite formation. The position of few significant peaks and observed characteristic bands of all

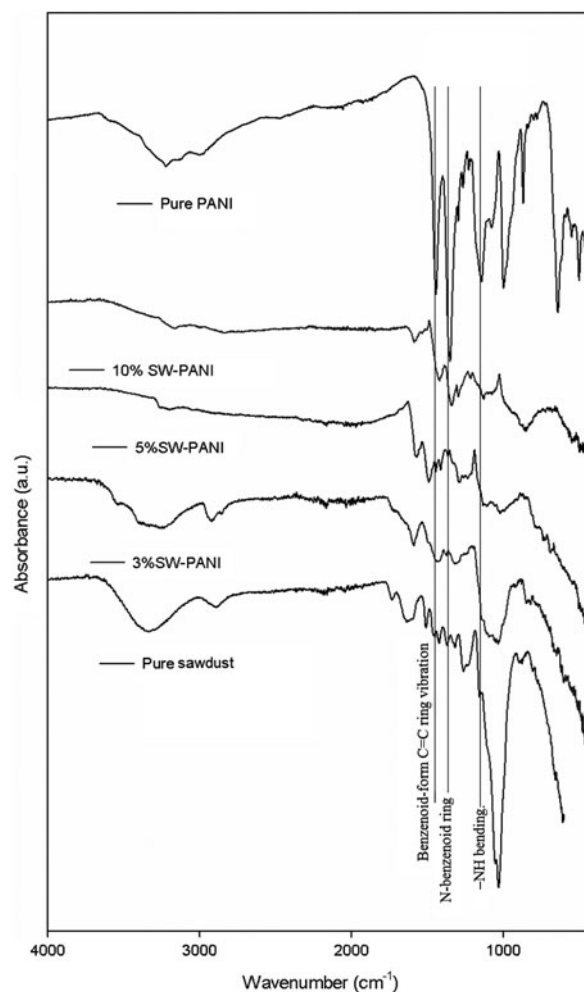


Fig. 2. FTIR spectra of pure PANI, pure sawdust and PANI–sawdust composites.

samples are marked in the figure. The obtained values are in good agreement with theoretical prediction [23].

### 3.3. UV–vis spectroscopy

UV–vis spectroscopy is a very sensitive tool for studying PANI protonation and more precisely, for the elucidation of the interactions between the solvent, doping anion and the polymer chain. The UV–vis spectrum of PANI shows two absorption peaks at 280 and 400 nm (Fig. 3) that are assigned to the  $\pi$ – $\pi^*$  transition and polarons band transitions, respectively. Another broad absorption shoulder is observed at the beginning of 630 nm that is ascribed to an excitonic transition in the quinoid ring [23].

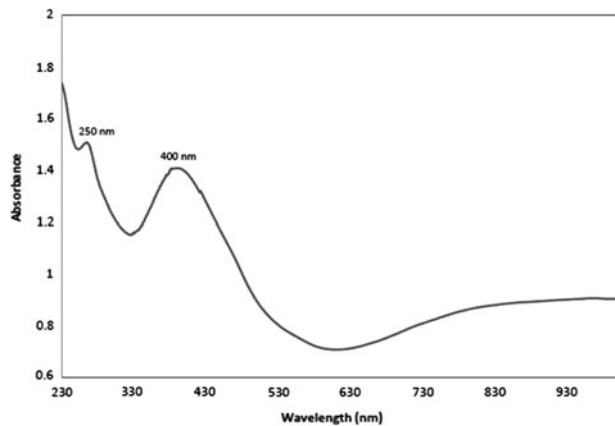


Fig. 3. UV-vis spectrum for the conducting form of pure PANI.

### 3.4. DSC measurements

Fig. 4 describes the DSC thermograms of pure PANI and PANI-sawdust composites with 3, 5 and 10% sawdust. The DSC measurement is performed in three steps: (1) all of the polymers and their composites are heated from room temperature (RT) until 100°C, (2) the sample is cooled from 100°C to RT and (3) the sample is heated from RT to 250°C. The thermograms of step 1 show an endothermic peak below 100°C due to the elimination of water and impurities; this peak also appears in the TGA thermograms. No significant changes are observed during the second step of DSC, whereas significant peaks with difference in regard to position and height are observed in the final step. Pure PANI shows two endothermic peaks, one at approximately 130°C, and the other at 240°C.

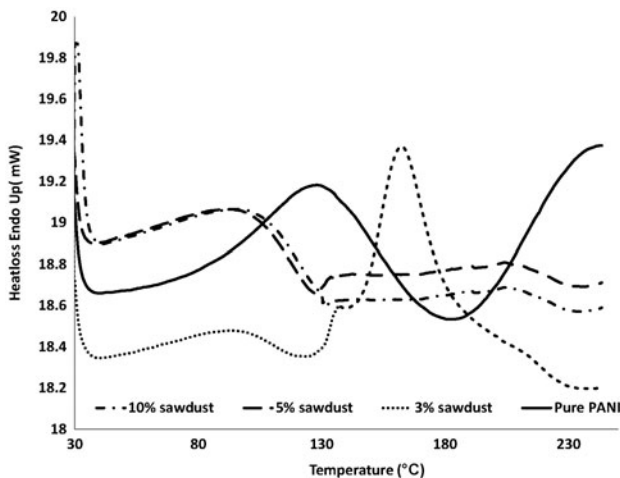


Fig. 4. DSC thermograms for pure PANI and for 3, 5 and 10% PANI-sawdust composites.

No melting peak is observed for PANI although it can exhibit some crystallinity and PANI's degradation temperature is lower than its melting temperature [23]. It is clear from the data that the composite films exhibit the combined physical properties of the polymer components.

### 3.5. TGA measurements

Fig. 5 illustrates the TGA of pure PANI and 3, 5 and 10% PANI-sawdust composites. The measurements are performed in the range of 30–700°C at a heating rate of 10°C/min. The TGA of pure PANI salt shows a three-step weight loss. The weight loss in the first step starts at approximately 70°C and continues up to 135°C due to the presence of moisture, which is used as a solvent in the preparation of PANI, free HCl and unreacted monomers. The second step may be attributed to the loss of dopants from deeper sites in the material. The major weight loss of chemically synthesised PANI-HCl at approximately 150–220°C is attributed to HCl loss. In the third step, the slow and gradual weight loss profile observed for the PANI salt at 220–380°C is due to polymer backbone degradation [26–28]. The TGA studies of sawdust reveal that the

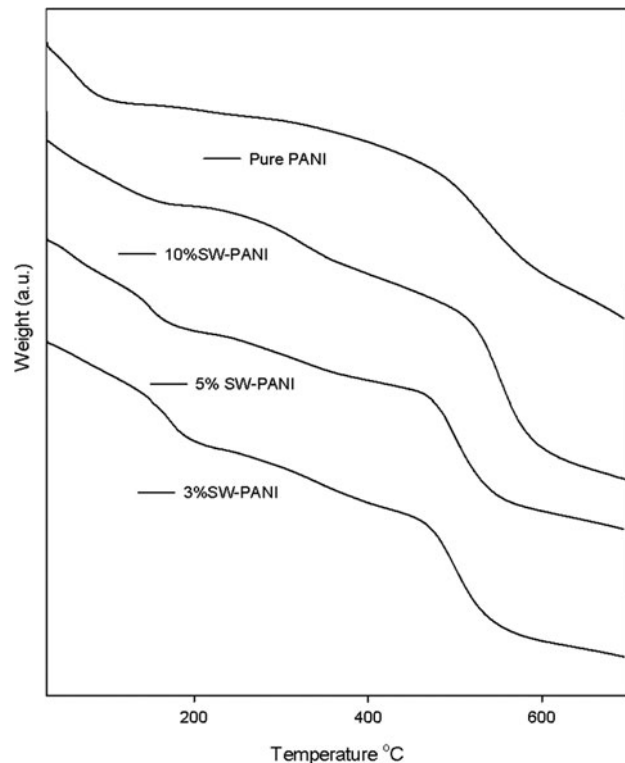


Fig. 5. TGA thermograms for pure PANI and for 3, 5 and 10% PANI-sawdust composites.

sawdust backbone is stable up to 275°C; its degradation commences near 300°C and completes at approximately 470°C. The TGA data of all of the composites show a four-step weight loss including the ranges similar to those of pure PANI.

### 3.6. Adsorption test

Adsorption tests for pure PANI and PANI–sawdust composites are performed and the results are listed in Table 1. The results indicate that PANI–5% sawdust composite has the best Pb removal efficiency; consequently, the remaining adsorption studies are accomplished for this particular composite only.

#### 3.6.1. Adsorption mechanism

The principle of adsorption mechanism can be demonstrated as: in PANI, the molecular structure of nitrogen acts as a connector between alternating benzenoid and quinoid rings. These nitrogen atoms in PANI behave as adsorption sites for Pb ions. The schematic diagrams in Figs. 6a and 6b describe the probable formation of different number of adsorption sites due to addition of various percentages of sawdust during composites formation. For the 3% composites, the interparticular gaps are quite large. As a result, most of the Pb-contaminated waste water passes through the system unfiltered and has the least removal efficiency (Table 1). In the cases of 5 and 10% PANI–sawdust composites, the pore sizes are big enough so that whole filtration of the Pb-contaminated wastewater goes assessed through the composite system. However, for 10% PANI–sawdust composites, most of the adsorption sites are covered; as increased content of sawdust significantly reduces exposed active surfaces for adsorption, so the removal efficiency has gone down consequently. Composite with 5% PANI–sawdust does have the highest number of exposed adsorption sites showing the highest adsorption efficiency. The results presented in Sections 3.1 and 3.7 justify the above arguments. Another

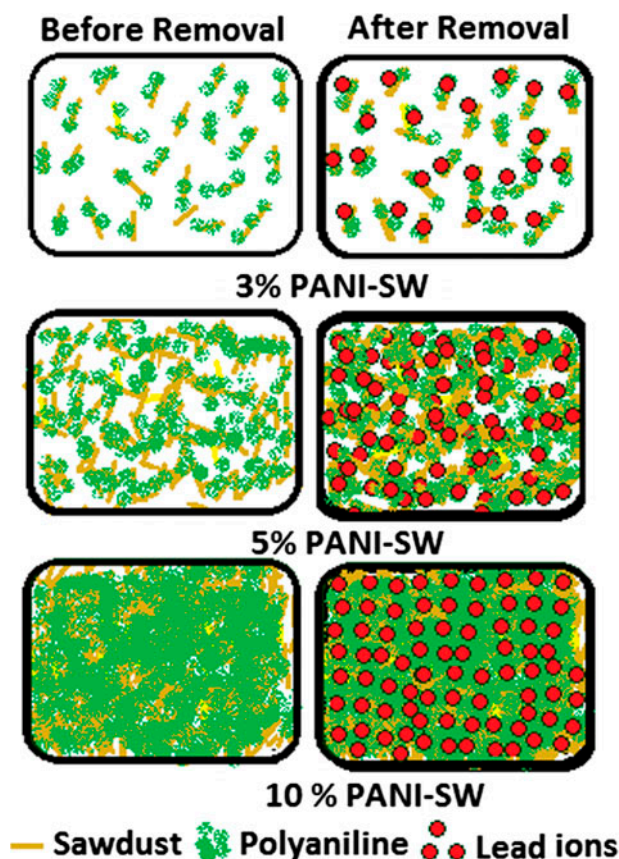


Fig. 6a. Schematic diagram of the mechanism of the composite formation and adsorption sites for lead ions on different PANI–sawdust composites.

schematic diagram presented in Fig. 6b describes the anticipated adsorption mechanism of Pb ions on the surface of PANI–sawdust composite. The process of ion exchange between Pb ions and amine group of anilinium ion is observed to be responsible for adsorption.

In order to explore adsorption process of heavy metal ions, a systematic study on the variables affecting the process are conducted further. The effects of various parameters such as time, pH, metal loading and composite dosages are taken into consideration.

#### 3.6.2. Effect of contact time

The effect of time on the adsorption process of PANI–5% sawdust nanocomposite is obtained by plotting the Pb removal efficiency as a function of time (shown in Fig. 7), where we take 0.2 g of PANI composites and 50 ppm Pb-contaminated solution with pH 5. It is found from the results that within 3 min of contact time, maximum adsorption is reached and this has the

Table 1  
Results of the adsorption tests

Sample	Removal efficiency (%)
Pure PANI	47
PANI–3% sawdust	53
PANI–5% sawdust	81
PANI–10% sawdust	56

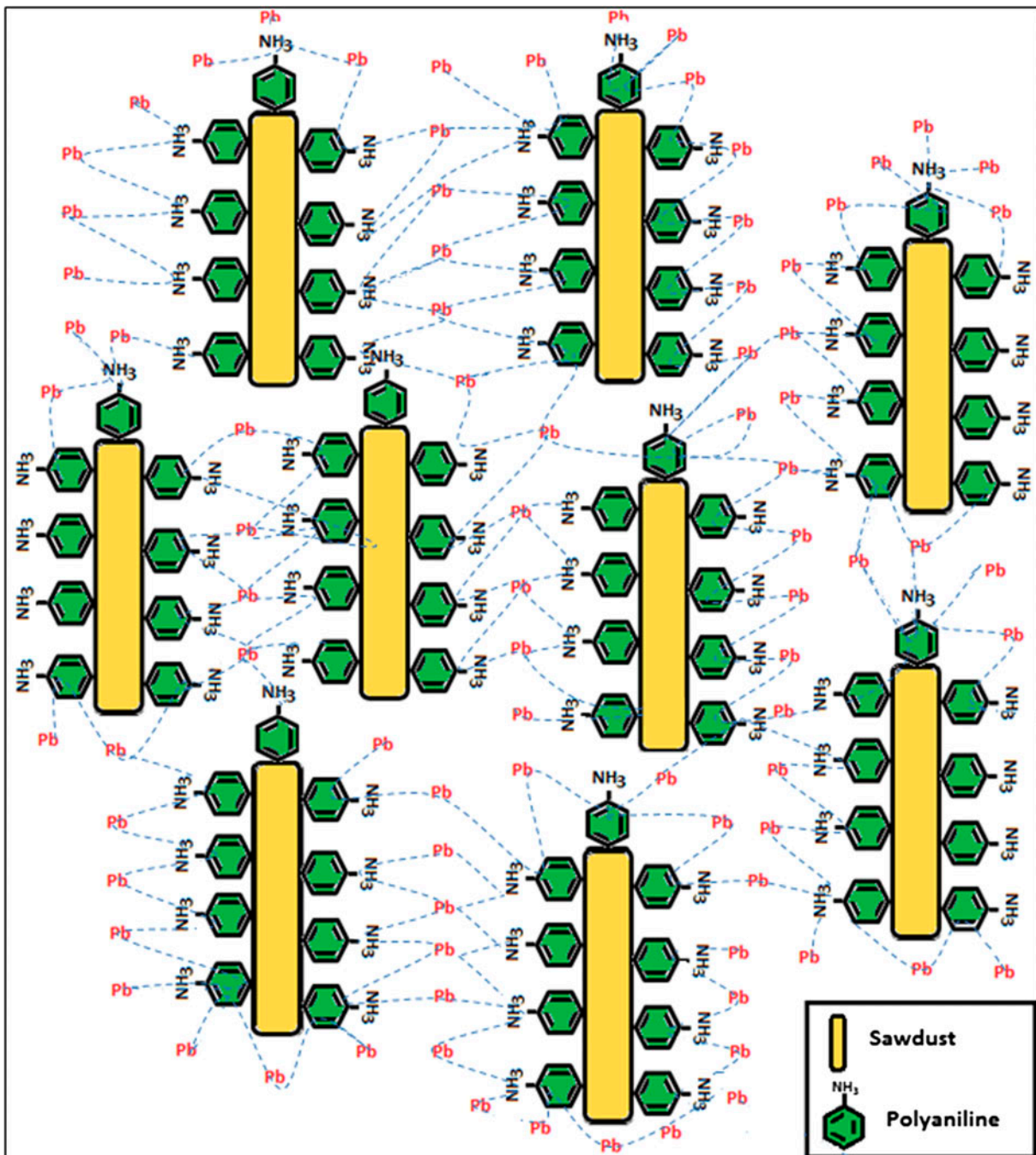


Fig. 6b. Schematic diagram showing ion exchange process between Pb and amine ions.

potential to remove up to 80% of the metal ion. The kinetics of metal ion adsorption is related to the interaction between metal ions and polymer composite matrix.

### 3.6.3. Effect of pH

The study highlighting the effect of pH on adsorption process of the nanocomposites is illustrated in

Fig. 8, in which removal coefficient is plotted over the pH (pH range 2–9) using 0.2 g of PANI nanocomposite and 50 ppm Pb solution. From the result, it is observed that the maximum adsorption of metal ions has occurred in case of solution with pH range 2–6 and decreased with further increase in pH. The pH of the solutions has shown a significant effect on the adsorption process. In this experiment, we keep the

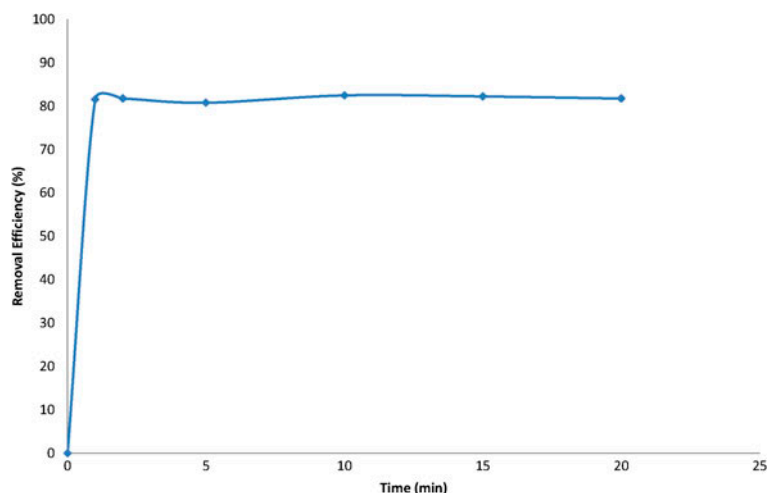


Fig. 7. Plot of removal efficiency vs. time for the PANI-5% sawdust composite.

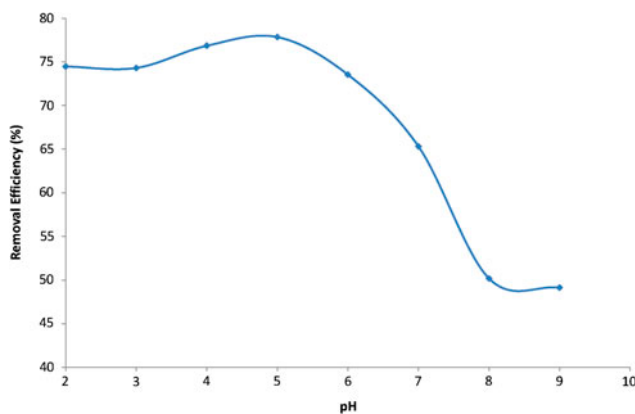


Fig. 8. Plot of removal efficiency vs. pH for the PANI-5% sawdust composite.

Pb solution's pH value as 5 in all these studies (Sections 3.6.2–3.6.4).

#### 3.6.4. Effect of metal loading

In order to investigate the polymer nanocomposite threshold limit of metal removal efficiency, the solutions with different concentrations of metal ions are analysed. The concentration range of metal ion chosen for this purpose varies from 30 to 100 ppm. The adsorption curve, shown in Fig. 9, indicates rapid increase in the removal efficiency for lower concentrations of Pb until 80 ppm. Beyond this concentration, the rate of increase is slow; the reason might be due to saturation of adsorption sites.

#### 3.6.5. Effect of composite dosage

Fig. 10 illustrates the weight effect of PANI composites on the adsorption of the metal ions. Varying amounts (0.1–0.5 g) of adsorbent are added in 100 mL of 50 ppm Pb solution under optimised conditions. From the graph, it is evident that the removal efficiency increases with increase in composite weight; it is an obvious fact because the increase in adsorbent concentration provides greater surface area for adsorption and as a result, it can hold more metal particles. In order to fit these data in two different mathematical models (described in next section), the action of adsorption isotherms on metal adsorption is studied.

#### 3.6.6. Adsorption isotherms

The adsorption isotherm for removal of Pb ion is studied using adsorbent dosage between 100 and 500 mg in 100 mL of aqueous solution containing 50 ppm Pb ions. The adsorption isotherms illustrate adsorption data that correlate with the relationship between two parameters at constant temperature, the amount of solute adsorbed per unit mass of adsorbent ( $a_e$ ) and the amount solution at equilibrium ( $c_e$ ). The adsorption data have been fitted using two adsorption isotherms, namely Freundlich adsorption isotherm and Langmuir adsorption isotherm.

**3.6.6.1. Freundlich adsorption isotherm.** The Freundlich adsorption isotherm is represented by the following equation:

$$a_e = k_F c_e^{1/n} \quad (2)$$

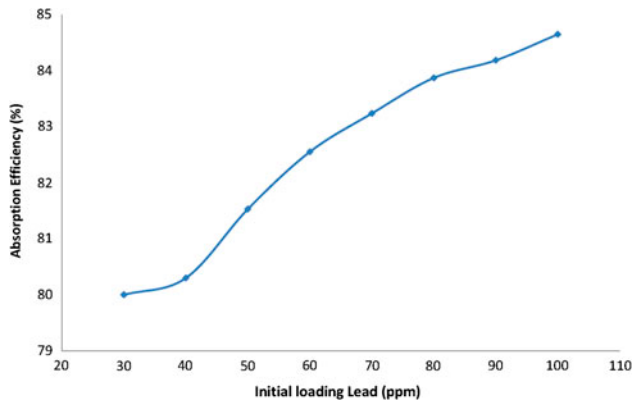


Fig. 9. Plot of removal efficiency vs. metal loading for the PANI-5% sawdust composite.

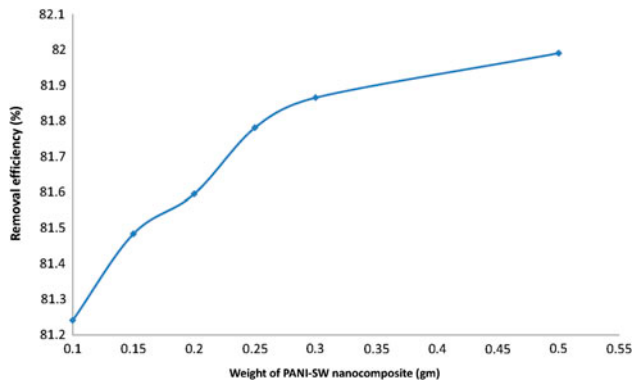


Fig. 10. Plot of removal efficiency vs. nanocomposite dosages for the PANI-5% sawdust composite.

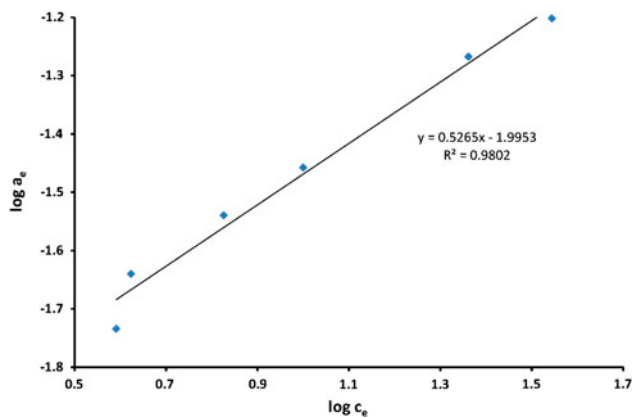


Fig. 11. Freundlich plot for the adsorption of lead by 5% PANI-sawdust composite.

where  $k_F$  and  $1/n$  are the Freundlich constants corresponding to the adsorption capacity and intensity of adsorption, respectively [29,30]. The logarithmic form of Eq. (2) in order to get its linear form is:

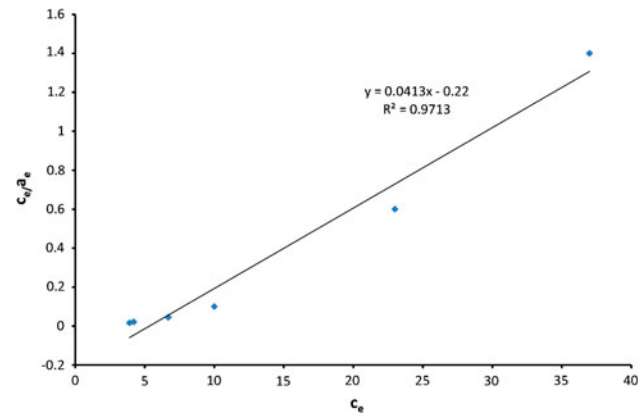


Fig. 12. Langmuir plot for the adsorption of lead 5% PANI-sawdust composite.

$$\log a_e = \log k_F + \frac{1}{n} \log c_e \quad (3)$$

A linear Freundlich plot is shown in Fig. 11 with  $R^2$  value of 0.98 justifying the validity of the system. The values of the Freundlich constants are obtained from the straight line plot,  $1/n$  from the slope and  $\log k_F$  from the intercept. The values are found to be 1.9 and 0.3, respectively. The fractional value of  $(1/n)$  indicates that the surface of adsorbent is of the heterogeneous with an exponential distribution of energy sites in other words, it indicates favourable adsorption of Pb on the surface of PANI nanocomposites. Furthermore, a relatively big value of  $k_F$ , justifies the high affinity of Pb species for the PANI nanocomposite conditions.

**3.6.6.2. Langmuir adsorption isotherm.** The parameters such as the quantity of solute adsorbed per unit mass of adsorbent ( $a_e$ ) and the amount of solution at equilibrium ( $c_e$ ), are fitted to the Langmuir adsorption isotherm for the monolayer [28–31]. Following equation represents the isotherm:

$$\frac{c_e}{a_e} = \frac{1}{bq_m} + \frac{c_e}{q_m} \quad (4)$$

From the linear plot of  $c_e/a_e$  vs.  $c_e$  shown in Fig. 12, value of the Langmuir constants such as maximum amount of metal ions adsorbed  $q_m$  (mg/g) and capacity of free energy of adsorption  $b$  (L/mg), are obtained from the slope and intercept of the fitted curve.

All the results of Freundlich and Langmuir isotherm are summarised in Table 2. From the results it is clear that the experimental values of  $c_e$  and  $a_e$  fits

Table 2

Adsorption isotherms equations and results for 5% PANI–sawdust composites

$R^2$	Constant-1	Constant-2
Freundlich equation: $\log a_c = \log k_F + \frac{1}{n} \log c_c$ : $y = 0.5265x - 1.9953$ 0.9802	$k_F = 0.3$	$n = 1.89$
Langmuir equation: $\frac{c_c}{a_c} = \frac{1}{bq_m} + \frac{c_c}{q_m}$ : $y = 0.0413x - 0.22$ 0.9713	$q_m = 24.21$	$b = -0.19$

well for the Freundlich isotherm then the Langmuir isotherm indicating that nanocomposite system has heterolayered structure.

### 3.7. Positron annihilation

The analysis of the collected positron lifetime spectra shows one main lifetime component in all samples (pure PANI and PANI–sawdust composites) with a high intensity in the range 97–99%. This lifetime ranges from 0.31 to 0.34 ns and it is possible due to positron annihilation in PANI matrix. Another lifetime (long) component having values between 1.1 and 1.3 ns with intensity (low) of 0.74–2.6% also appears in the analysis of the spectra. No significant change in lifetime components is observed in both the cases, before and after Pb removal from aqueous solutions. However, changes are observed in the intensities of these lifetimes as shown in Fig. 13 for the intensity of the long-lived component. Before Pb removal, the intensity that is linked with the concentration of open volumes in the sample increases with increase in concentration of sawdust particles to reach maximum value in case of 5% sawdust composite and then it

decreases for 10% sawdust composite. This behaviour is consistent with the morphology of samples revealed by SEM (Fig. 1) results, where more vacancies are observed in 5% sawdust composite as compared with the large but less open areas in 3% sawdust composite or the homogenous structure of the well-bounded sawdust particles with PANI matrix in the 10% sawdust composite.

However, the intensity of same long lifetime component after Pb removal is slightly higher than the case before Pb removal in pure PANI and 3% sawdust composite, perhaps due to the formation of some open-volume defects upon introducing Pb particles. Subsequently, it decreases for the 5 and 10% sawdust composites. This decrease in intensity of long lifetime component could probably be attributed to the adsorption of Pb particles in open volumes of the composites (and hence smaller number and/or size of the composite particles), which explains the slight decay in lifetime after Pb removal as compared to that of the case before Pb removal. These observations are in good agreement with the results of other characterisation techniques, where the efficiency of Pb removal is found better with an increase in the concentration of sawdust particles in the composites.

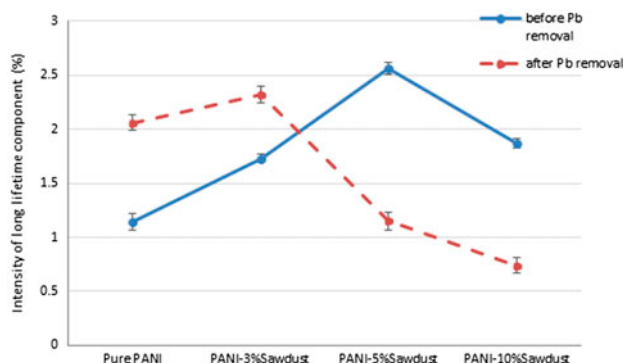


Fig. 13. Variation of the intensity of the long positron lifetime component for pure PANI and for the 3, 5 and 10% PANI–sawdust composites.

## 4. Conclusion

In this paper, three different concentrations of PANI–sawdust nanocomposites are synthesised via casting method at room temperature in aqueous media. The ability of these composites to remove Pb ion from aqueous solution is investigated. The morphological and structural characteristics of the nanocomposites are studied. It is found that adding sawdust particles increases the size and density of the composites' particles. The molecular structure of the composites is determined using FTIR spectroscopy. Adsorption experiments are performed for the removal of Pb ions from aqueous solution. The adsorption characteristics are tested at different pH

values and contact time. The results indicate that the 5% PANI–sawdust nanocomposite has considerable ability to remove Pb ions from aqueous solution. Optimum conditions for Pb removal are found at pH 5 and equilibrium time of 3 min. Positron annihilation measurement confirms the adsorption of the Pb ions by the composites and explains the structural changes of the composites upon Pb adsorption.

### Acknowledgement

This work is a piece of project awarded by the Undergraduate Research Experience Program (UREP) grant, Qatar National Research Fund (QNRF), #UREP 14-113-1-015. The statements made herein are solely the responsibility of the author(s).

### References

- [1] N. Ayawei, A.K. Inengite, D. Wankasi, E.D. Dikio, Synthesis and sorption studies of lead(II) on Zn/Fe layered double hydroxide, *Am. J. Appl. Chem.* 3 (2015) 124–133.
- [2] R. Karthik, S. Meenakshi, Adsorption study on removal of Cr(VI) ions by polyaniline composite, *Desalin. Water Treat.* 54 (2015) 3083–3093.
- [3] M.H. Qomi, H. Eisazadeh, M. Hosseini, H.A. Namaghi, Manganese removal from aqueous media using polyaniline nanocomposite coated on wood sawdust, *Synth. Met.* 194 (2014) 153–159.
- [4] M.A.A. Zaini, Y. Amano, M. Machida, Adsorption of heavy metals onto activated carbons derived from polyacrylonitrile fiber, *J. Hazard. Mater.* 180 (2010) 552–560.
- [5] I.E. Mejias Carpio, J.D. Mangadlao, H.N. Nguyen, R.C. Advincula, D.F. Rodrigues, Graphene oxide functionalized with ethylenediamine triacetic acid for heavy metal adsorption and anti-microbial applications, *Carbon* 77 (2014) 289–301.
- [6] S. Mandal, M.K. Sahu, R.K. Patel, Adsorption studies of arsenic(III) removal from water by zirconium polyacrylamide hybrid material (ZrPACM-43), *Water Resour. Ind.* 4 (2013) 51–67.
- [7] T.F. Otero, I. Cantero, Conducting polymers as positive electrodes in rechargeable lithium-ion batteries, *J. Power Sources* 81–82 (1999) 838–841.
- [8] Y. Wang, X. Jing, Intrinsically conducting polymers for electromagnetic interference shielding, *Polym. Adv. Technol.* 16 (2005) 344–351.
- [9] Y. Lin, W. Cai, X. Tian, X. Liu, G. Wang, C. Liang, Polyacrylonitrile/ferrous chloride composite porous nanofibers and their strong Cr-removal performance, *J. Mater. Chem.* 21 (2011) 991–997.
- [10] B. Davodi, M. Jahangiri, Determination of optimum conditions for removal of As(III) and As(V) by polyaniline/polystyrene nanocomposite, *Synth. Met.* 194 (2014) 97–101.
- [11] R.A. Salih, Synthesis, identification and study of electrical conductivity of the doped poly aniline, *Arabian J. Chem.* 3 (2010) 155–158.
- [12] S. Bhadra, D. Khastgir, N.K. Singha, J.H. Lee, Progress in preparation, processing and applications of polyaniline, *Prog. Polym. Sci.* 34 (2009) 783–810.
- [13] C.W. Lee, S.H. Choi, H.M. Jeong, S.H. Rhyu, K.W. Chi, K.S. Yoon, Synthesis of tailor-made nanoporous polyaniline derived with PVA/alkaline metal system for metal complexation, *J. Appl. Polym. Sci.* 122 (2011) 2497–2502.
- [14] B.L. Lee, Electrically conductive polymer composites and blends, *Polym. Eng. Sci.* 32 (1992) 36–42.
- [15] O. Turkarlan, M. Ak, C. Tanyeli, I.M. Akhmedov, L. Toppare, Enhancing electrochromic properties of conducting polymers via copolymerization: Copolymer of 1-(4-fluorophenyl)-2,5-di(thiophen-2-yl)-1H-pyrrole with 3,4-ethylene dioxothiophene, *J. Polym. Sci., Part A: Polym. Chem.* 45 (2007) 4496–4503.
- [16] G. Li, Y. Li, H. Peng, Y. Qin, Synthesis and electrochemical performances of dispersible polyaniline/sulfonated graphene composite nanosheets, *Synth. Met.* 184 (2013) 10–15.
- [17] M.B. Keivani, K. Zare, H. Aghaie, R. Ansari, Removal of methylene blue dye by application of polyaniline nano composite from aqueous solutions, *J. Phys. Theor. Chem. Islamic Azad Univ. Iran* 6 (2009) 50–56.
- [18] R. Ansari, H. Dezhampah, Application of polyaniline/sawdust composite for removal of acid green 25 from aqueous solutions: Kinetics and thermodynamic studies, *Eur. Chem. Bull.* 2 (2013) 220–225.
- [19] R. Ansari, M.B. Keivani, A.F. Delavar, Application of polyaniline nanolayer composite for removal of tartrazine dye from aqueous solutions, *J. Polym. Res.* 18 (2011) 1931–1939.
- [20] D. Zareyee, H. Tayebi, S. H. Javadi, Preparation of polyaniline/activated carbon composite for removal of reactive red 198 from aqueous solution, *Iranian, J. Org. Chem.* 4 (2012) 799–802.
- [21] R. Ansari, Application of polyaniline and its composites for adsorption/recovery of chromium(VI) from aqueous solutions, *Acta Chim. Slov.* 53 (2006) 88–94.
- [22] F. Kanwal, R. Rehman, J. Anwar, T. Mahmud, Adsorption studies of cadmium(II) using novel composites of polyaniline with rice husk and saw dust of *Eucalyptus camaldulensis*, *Electron. J. Environ., Agric. Food Chem.* 10 (2011) 2972–2985.
- [23] J. Bhadra, N.K. Madi, N.J. Al-Thani, M.A. Al-Maadeed, Polyaniline/polyvinyl alcohol blends: Effect of sulfonic acid dopants on microstructural, optical, thermal and electrical properties, *Synth. Met.* 191 (2014) 126–134.
- [24] J. Stejskal, R.G. Gilbert, Polyaniline. Preparation of a conducting polymer, *Pure Appl. Chem.* 74 (2002) 857–867.
- [25] J. Kansy, Microcomputer program for analysis of positron annihilation lifetime spectra, *Nucl. Instrum. Methods Phys. Res., Sect. A* 374 (1996) 235–244.
- [26] S. Palaniappan, B.H. Narayana, Conducting polyaniline salts: Thermogravimetric and differential thermal analysis, *Thermochim. Acta* 237 (1994) 91–97.
- [27] S.H. Hosseini, A.A. Entezami, Preparation and characterization of polyaniline blends with polyvinyl acetate, polystyrene and polyvinyl chloride for toxic gas sensors, *Polym. Adv. Technol.* 12 (2001) 482–493.
- [28] R. Ansari, M.B. Keivani, Polyaniline conducting electroactive polymers: Thermal and environmental stability studies, *E-J. Chem.* 3 (2006) 202–217.

- [29] A. Rashidzadeh, A. Olad, Novel polyaniline/poly (vinyl alcohol)/clinoptilolite nanocomposite: Dye removal, kinetic, and isotherm studies, *Desalin. Water Treat.* 51 (2013) 7057–7066.
- [30] R. Kumar, M.O. Ansari, M.A. Barakat, Adsorption of brilliant green by surfactant doped polyaniline/MWCNTs composite: Evaluation of the kinetic, thermodynamic, and isotherm, *Ind. Eng. Chem. Res.* 53 (2014) 7167–7175.
- [31] A. Olad, F.F. Azhar, A study on the adsorption of chromium(VI) from aqueous solutions on the alginate-montmorillonite/polyaniline nanocomposite, *Desalin. Water Treat.* 52 (2014) 2548–2559.